American Mineralogist, Volume 85, pages 770–777, 2000

Comparative high-pressure crystal chemistry of wadsleyite, β-$(Mg_{1-x}Fe_x)_2SiO_4$, with $x = 0$ and 0.25

ROBERT M. HAZEN,* MICHELLE B. WEINBERGER, HEXIONG YANG, AND CHARLES T. PREWITT

Geophysical Laboratory and Center for High Pressure Research, Carnegie Institution of Washington, 5251 Broad Branch Road, N.W., Washington, D.C. 20015-1305, U.S.A.

ABSTRACT

High-pressure crystal structures are reported for two synthetic wadsleyite crystals, β-Mg_2SiO_4 (Fe00) and β-$(Mg_{0.75}Fe_{0.25})_2SiO_4$ (Fe25), at six pressures to 10.12 GPa. In both compositions, bulk compressibilities are equal to the average compressibility of divalent cation octahedra. Individual silicate tetrahedra, by contrast, are relatively rigid, though the Si-O-Si angle between tetrahedra in Si_2O_7 dimers decreases systematically with pressure. Wadsleyites display anisotropic compression, with the *c* axis approximately 40% more compressible than *a* or *b*. This behavior results from differential compression of (Mg,Fe)-O bonds; in each of the structure's three symmetrically independent octahedra, the longest and most compressible bonds are roughly parallel to the *b* axis. Although the linear compressibilities of Fe00 and Fe25 are similar, details of structural changes with pressure differ. Iron-enriched M1 and M3 octahedral sites in Fe25 are significantly less compressible than analogous Mg sites in Fe00.

INTRODUCTION

Wadsleyite, β-$(Mg,Fe)_2SiO_4$, is stable between the phase fields of olivine (the lower pressure α form) and ringwoodite (the higher pressure γ form) and is thought to be a major mineral in the upper portion of the transition zone of a peridotitic mantle (e.g., Anderson 1970; Jeanloz and Thompson 1983; Bina and Wood 1987). Because the α-to-β phase transformation is believed to be responsible for the 410 km discontinuity observed in seismic velocity-depth profiles, the crystal-chemical and physical properties of wadsleyite have been a central subject of a variety of experimental studies. Recent work includes structure refinements (Finger et al. 1993 and references therein), compressibility measurements (Mizukami et al. 1975; Hazen et al. 1990; Fei et al. 1992), thermal expansion and high-temperature structure refinements (Tsukimura et al. 1988; Reynard et al. 1996), high-pressure infrared and Raman spectroscopy (Williams et al. 1986; Chopelas 1991; Cynn and Hofmeister 1994), ultrasonic studies (Gwanmesia et al. 1990; Li et al. 1996, 1998) and Brillouin spectroscopy (Sawamoto et al. 1984; Zha et al. 1997). Moreover, recent theoretical (Smyth 1987, 1994; Downs 1989; Haiber et al. 1997) and experimental (McMillan et al. 1991; Bell and Rossman 1992; Gasparik 1993; Young et al. 1993; Inoue 1994; Kudoh et al. 1996; Kudoh and Inoue 1999) studies have shown that wadsleyite may contain significant H, suggesting that it could serve as a major host for H_2O in the mantle. The saturation concentration of H_2O in wadsleyite is estimated to be as much as ~3.3 wt%.

The orthorhombic crystal structure (space group *Imma*) of the β-phase consists of three symmetrically independent octahedral sites (M1, M2, and M3) and one tetrahedral site (T). Details of the structure were first determined by Morimoto et al. (1969) from a β-Mn_2GeO_4 single crystal and by Moore and Smith (1970) from a polycrystalline sample of β-$(Mg_{0.9}Ni_{0.1})_2SiO_4$. Further structure refinements on β-Mn_2GeO_4 and β-Co_2SiO_4 were conducted by Morimoto et al. (1970, 1974). The β-Mg_2SiO_4 structure was refined by Horiuchi and Sawamoto (1981). Sawamoto and Horiuchi (1990) investigated the crystal structure of β-$(Mg_{0.9}Fe_{0.1})_2SiO_4$ and reported the preference of Fe^{2+} for the M1 and M3 octahedral sites over the M2 site. A similar result was observed by Finger et al. (1993) from structure refinements of five β-$(Mg_{1-x}Fe_x)_2SiO_4$ crystals with *x* ranging from 0 to 0.4.

Several recent studies have described variants of the wadsleyite structure. Kudoh et al. (1996) and Kudoh and Inoue (1999) refined hydrous wadsleyite structures ($Mg_{2-x}SiH_{2x}O_4$) with orthorhombic *Immm* symmetry, whereas Smyth et al. (1997) reported a hydrous wadsleyite structure ($Mg_{1.73}Fe_{0.10}Al_{0.10}Si_{0.99}H_{0.36}O_4$) with monoclinic *I*2/*m* symmetry. Woodland and Angel (1998) studied the crystal structure of β-$(Fe^{2+}_{1.55}Fe^{3+}_{0.45})(Si_{0.55}Fe^{3+}_{0.45})O_4$ synthesized at 5.6 GPa and 1100 °C and noted that Fe^{3+} prefers the M1 and M3 sites over the M2 site.

In this paper, we present an X-ray structure study of two β-$(Mg_{1-x}Fe_x)_2SiO_4$ crystals, with $x = 0.00$ and 0.25, at various pressures to 10.1 GPa using the comparative high-pressure method (Hazen 1993) to investigate the compression behavior of wadsleyite, as well as the effects of Fe on the β-phase structure at high pressures.

EXPERIMENTAL PROCEDURES

Both β-Mg_2SiO_4 and β-$(Mg_{0.75}Fe_{0.25})_2SiO_4$ samples (designated as Fe00 and Fe25, respectively) used in this study were synthesized in the High-Pressure Laboratory of SUNY at Stony Brook, as reported by Finger et al. (1993). The Fe00 sample was previously studied by Zha et al. (1997), who determined

*E-mail: hazen@gl.ciw.edu

TABLE 1. Crystal data and other relevant information on β-phase at various pressures

P (GPa)	*a* (A)	*b* (A)	*c* (A)	*V* (A³)	Refls.>3σ (*I*)	R_{int}*	R_w†	*R*‡
				Fe00				
0.00	5.6978(4)	11.4620(5)	8.2571(5)	539.26(4)	236	0.028	0.036	0.045
1.30§	5.6854(4)	11.4368(5)	8.2323(4)	535.29(5)				
2.72	5.6731(4)	11.4114(4)	8.2067(4)	531.29(4)	246	0.033	0.035	0.043
3.83§	5.6629(4)	11.3902(5)	8.1852(4)	527.95(4)				
5.23	5.6515(4)	11.3688(5)	8.1630(4)	524.48(4)	247	0.030	0.037	0.044
6.80	5.6390(3)	11.3432(4)	8.1389(4)	520.60(4)	241	0.033	0.036	0.044
8.49	5.6261(4)	11.3158(6)	8.1132(5)	516.51(5)	238	0.029	0.035	0.043
10.12	5.6137(4)	11.2918(5)	8.0895(4)	512.79(5)	239	0.026	0.038	0.046
				Fe25				
0.00	5.7194(6)	11.5114(8)	8.3021(5)	546.59(6)	230	0.031	0.035	0.043
1.30§	5.7075(6)	11.4854(6)	8.2768(4)	542.56(6)				
2.72	5.6951(5)	11.4628(4)	8.2515(4)	538.67(5)	223	0.033	0.032	0.038
3.83§	5.6846(6)	11.4421(6)	8.2303(4)	535.33(6)				
5.23	5.6737(5)	11.4201(5)	8.2082(3)	531.85(5)	232	0.032	0.032	0.046
6.80	5.6605(5)	11.3940(5)	8.1828(4)	527.76(5)	229	0.034	0.037	0.047
8.49	5.6485(5)	11.3707(5)	8.1594(3)	524.05(5)	232	0.035	0.038	0.047
10.12	5.6365(4)	11.3464(5)	8.1358(3)	520.31(5)	229	0.029	0.035	0.046

* Residual for internal agreement of symmetry equivalent reflections.
† $R_w = (\Sigma w(F_o - F_c)^2 / \Sigma wFo^2)^{0.5}$.
‡ $R = \Sigma|F_o - F_c| / \Sigma|F_o|$.
§ X-ray intensity data were not collected at these pressures.

elastic constants. They also examined the sample with Raman spectroscopy and detected no peaks characteristic of hydroxyl. The Fe25 sample was used by Hazen et al. (1990) for comparative compressibility measurements and by Finger et al. (1993) for structure refinement, which shows that the site occupancies of Fe in the M1, M2, and M3 sites are 0.288(4), 0.132(4), and 0.290(4), respectively.

In this study, the two crystals were mounted together in a modified Merrill-Bassett diamond-anvil cell with a mixture of 4:1 methanol:ethanol as the pressure medium. Four ruby chips (<10 μm) were included as the internal pressure calibrant (Mao et al. 1986), from which pressure was determined from the position of the R_1 laser-induced fluorescence peak, with an error of approximately ±0.05 GPa.

A Picker four-circle diffractometer equipped with a Mo X-ray tube (β-filtered; λ = 0.70930 Å) was used for all X-ray diffraction measurements. The fixed-φ mode of data measurement (Finger and King 1978) was employed throughout the high-pressure experiments to maximize reflection accessibility and minimize attenuation by the diamond cell. Unit-cell parameters were determined by fitting the positions of 14 to18 reflections with 20° < 2θ < 35°, following the procedure of King and Finger (1979). X-ray diffraction intensity data were collected on the basis of the *I*-centered lattice for all accessible reflections with 0 < 2θ < 60° using ω scans of 1° width in step increments of 0.025° and 4-s per step counting time.

The intensity data were measured at six pressures up to 10.12 GPa. At 10.12 GPa, a set of intensity data with 0° < 2θ < 30° was also collected for both crystals based on the primitive lattice to check if any reflections violated the *Imma* symmetry; no such reflections were detected. Digitized step data were integrated by the method of Lehmann and Larsen (1974) with background manually reset when necessary. Corrections were made for Lorentz and polarization effects, and for X-ray absorption by the crystal. In addition, corrections were made for absorption by the diamond and beryllium components of the pressure cell. Reflections having intensities greater than 2σ(*I*) were considered as observed and were included in refinements, where σ(*I*) is the standard deviation determined from the counting statistics. Both ruby fluorescence peaks and X-ray diffraction peaks remained sharp to the highest pressure, suggesting that hydrostatic conditions were maintained.

The initial structural model of wadsleyite was taken from Finger et al. (1993). Least-squares refinements were carried out using an updated version of RFINE4 (Finger and Prince 1975) in space group *Imma*. Neutral atomic scattering factors, including anomalous dispersion corrections for Mg, Si, and O, were taken from Ibers and Hamilton (1974). For all high-pressure structure refinements, the Mg-Fe occupancies at the M1, M2, and M3 sites for Fe25 were assumed to be the same as those determined by Finger et al. (1993). Anisotropic refinements were made for all data sets of two samples. Weighting schemes were based on $w = [\sigma^2(F) + (pF)^2]^{-1}$, where *p* is adjusted to ensure that the errors were normally distributed through probability plot analysis (Ibers and Hamilton 1974). Type II isotropic extinction corrections (Becker and Coppens 1975) were applied in the refinements. Unit-cell dimensions and final refinement statistics are reported in Table 1. Atomic positional and isotropic displacement parameters are listed in Table 2; selected interatomic distances, along with polyhedral volumes and distortion indices, are presented in Table 3 and selected interatomic angles in Table 4.

RESULTS AND DISCUSSION

Linear compressibilities and bulk moduli

All unit-cell dimensions (*a*, *b*, *c*, and *V*) of both Fe00 and Fe25 decrease uniformly with increasing pressure. Furthermore, the corresponding cell parameters of the two samples exhibit similar compressibilities in the experimental pressure range, supporting the conclusion of Hazen et al. (1990) that the Fe content has little effect on the linear or bulk compressibilities of the wadsleyite structures. The linear compressibilities of the *a*, *b*, and *c* dimensions (β_a, β_b, and β_c) are 0.00145(2), 0.00146(3), and 0.00200(4)/GPa, respectively, for Fe00 with the axial compression ratios (β_a: β_b: β_c) of 0.99:1.00:1.37. Cor-

responding values for Fe25 are 0.00143(3), 0.00141(3), and 0.00197(5)/GPa, with (β_a: β_b: β_c) = 1.01:1.00:1.40. Hazen et al. (1990) attributed the relative stiffness of wadsleyite along the *a* and *b* axes to the pseudo-layering features of the structure, with (Mg,Fe)-octahedral layers parallel to the *a*-*b* plane, and cross-linking by Si_2O_7 dimers along the *c* axis. The axial compression ratios we obtained in this study are in excellent agreement with those determined from single-crystal X-ray diffraction (Hazen et al. 1990) as well as from Brillouin spectroscopy (Sawamoto et al. 1984; Zha et al. 1997).

We fit weighted unit-cell volume and weighted pressure data to a third-order Birch-Murnaghan equation of state to yield: V_0 = 539.26(9) Å^3, K_{T0} = 172(3) GPa, and $K'_{T0} = \partial K/\partial P$ = 6.3(7) for Fe00, and V_0 = 546.59(6) Å^3, K_{T0} = 173(3) GPa, and K'_{T0} = 7.1(8) for Fe25. These isothermal bulk moduli are comparable to the 172.5(10) and 170(2) GPa values obtained by Sawamoto et al. (1984) and Zha et al. (1997), respectively, from Brillouin-scattering measurements, and the 172(2) GPa value reported by Li et al. (1996, 1998) on single-crystal Fe00 wadsleyite. Single-crystal X-ray diffraction data up to 4.51 GPa reported by Hazen et al. (1990), and reanalyzed by Jeanloz and Hazen (1991) by means of finite-strain analysis, yield bulk moduli of 165(3) and 170(1) GPa for Fe00 and Fe25, respectively. Gwanmesia et al. (1990) report slightly lower bulk moduli of 164.4 to 168.8(8) GPa from ultrasonic measurements of polycrystalline Fe00 wadsleyite.

Values of $K'_{T0} > 6$ reported here, though not well constrained by only seven high-pressure data, are significantly greater than the $K'_{T0} < 5$ cited in several previous studies (Sawamoto et al. 1984; Gwanmesia et al. 1990; Jeanloz and Hazen 1991; Zha et al. 1997; Li et al. 1998). The reasons for these differences may reflect a gradual change in compression mechanisms with increasing pressure, or small, systematic errors in pressure calibration at the highest pressures of this study. These uncertainties do not affect the structural results of this study, but further equation-of-state measurements may be warranted.

Structural variations of β-Mg_2SiO_4 with pressure

The wadsleyite structure is based on close-packing of cation polyhedra and features extensive edge-sharing of divalent

TABLE 2. Atomic positional coordinates and isotropic displacement factors for $(Mg,Fe)_2SiO_4$ wadsleyite at various pressures

P (GPa)		0.00	2.72	5.23	6.80	8.49	10.12
				Fe00			
M1	B_{iso}	0.45(7)	0.47(7)	0.51(7)	0.43(7)	0.54(7)	0.49(7)
M2	*z*	0.9698(5)	0.9708(5)	0.9711(4)	0.9715(4)	0.9713(4)	0.9716(4)
	B_{iso}	0.46(6)	0.48(6)	0.48(6)	0.46(6)	0.43(6)	0.45(6)
M3	*y*	0.1269(3)	0.1274(2)	0.1273(2)	0.1273(2)	0.1275(2)	0.1270(2)
	B_{iso}	0.59(5)	0.57(4)	0.58(5)	0.56(4)	0.54(4)	0.52(5)
Si	*y*	0.1199(2)	0.1201(2)	0.1199(1)	0.1199(2)	0.1199(1)	0.1199(2)
	z	0.6165(2)	0.6170(2)	0.6170(2)	0.6173(2)	0.6173(2)	0.6173(2)
	B_{iso}	0.26(4)	0.27(4)	0.29(4)	0.30(3)	0.26(3)	0.26(4)
O1	*z*	0.2182(9)	0.2197(9)	0.2204(8)	0.2203(9)	0.2208(9)	0.2208(9)
	B_{iso}	0.47(11)	0.47(10)	0.48(12)	0.50(11)	0.47(10)	0.46(11)
O2	*z*	0.7157(8)	0.7162(8)	0.7184(7)	0.7173(8)	0.7192(8)	0.7201(8)
	B_{iso}	0.48(10)	0.53(10)	0.42(10)	0.44(10)	0.47(11)	0.41(10)
O3	*y*	0.9898(4)	0.9890(4)	0.9900(4)	0.9905(4)	0.9907(4)	0.9914(4)
	z	0.2565(7)	0.2557(8)	0.2549(6)	0.2546(7)	0.2550(7)	0.2545(7)
	B_{iso}	0.54(9)	0.50(9)	0.51(8)	0.53(9)	0.51(9)	0.46(10)
O4	*x*	0.2601(5)	0.2597(5)	0.2601(5)	0.2596(5)	0.2591(5)	0.2589(6)
	y	0.1226(4)	0.1216(4)	0.1226(3)	0.1221(3)	0.1222(3)	0.1228(4)
	z	0.9931(4)	0.9928(4)	0.9927(4)	0.9929(4)	0.9929(4)	0.9936(4)
	B_{iso}	0.46(6)	0.51(5)	0.56(6)	0.43(6)	0.49(6)	0.43(5)
				Fe25			
M1	B_{iso}	0.60(7)	0.68(7)	0.62(6)	0.51(6)	0.59(7)	0.48(6)
M2	*z*	0.9706(4)	0.9711(3)	0.9709(3)	0.9707(4)	0.9719(4)	0.9719(4)
	B_{iso}	0.64(7)	0.69(6)	0.52(6)	0.56(6)	0.67(7)	0.63(7)
M3	*y*	0.1255(2)	0.1254(2)	0.1256(2)	0.1253(2)	0.1257(2)	0.1254(2)
	B_{iso}	0.66(4)	0.58(5)	0.48(4)	0.50(4)	0.56(4)	0.61(4)
Si	*y*	0.1209(2)	0.1209(2)	0.1211(2)	0.1208(2)	0.1209(2)	0.1211(2)
	z	0.6166(3)	0.6170(2)	0.6171(2)	0.6172(2)	0.6171(2)	0.6175(2)
	B_{iso}	0.37(4)	0.31(3)	0.35(4)	0.35(4)	0.31(4)	0.31(4)
O1	*z*	0.2174(9)	0.2206(7)	0.2207(8)	0.2217(8)	0.2220(9)	0.2222(8)
	B_{iso}	0.64(15)	0.47(14)	0.63(12)	0.53(12)	0.54(12)	0.50(13)
O2	*z*	0.7163(9)	0.7179(7)	0.7184(7)	0.7187(8)	0.7193(8)	0.7198(8)
	B_{iso}	0.63(15)	0.54(13)	0.48(12)	0.52(12)	0.56(13)	0.49(14)
O3	*y*	0.9875(5)	0.9888(4)	0.9887(4)	0.9887(5)	0.9887(5)	0.9886(4)
	z	0.2563(7)	0.2565(6)	0.2554(6)	0.2556(7)	0.2542(7)	0.2544(6)
	B_{iso}	0.47(12)	0.66(11)	0.55(12)	0.67(11)	0.68(11)	0.58(11)
O4	*x*	0.2626(8)	0.2633(6)	0.2623(7)	0.2624(8)	0.2622(8)	0.2613(7)
	y	0.1231(5)	0.1232(6)	0.1239(4)	0.1238(4)	0.1247(4)	0.1248(4)
	z	0.9924(4)	0.9918(3)	0.9924(3)	0.9925(4)	0.9924(4)	0.9925(3)
	B_{iso}	0.53(7)	0.49(6)	0.53(6)	0.50(6)	0.47(7)	0.56(6)

Note: The following constraints apply to some atomic positional coordinates: $x = y = z = 0$ for M1; $x = 0$ and $y = 1/4$ for M2, O1, and O2; $x = z = 1/4$ for M3; $x = 0$ for Si and O3.

TABLE 3. Interatomic distances(A) and octahedral distortion indices of $(Mg,Fe)_2SiO_4$ Wadsleyite at various pressures

P(GPa)	0.00	2.72	5.23	6.80	8.49	10.12
			Fe00			
M1-O3 ×2	2.121(6)	2.102(7)	2.084(5)	2.075(6)	2.072(6)	2.061(6)
M1-O4 ×4	2.043(4)	2.025(4)	2.027(3)	2.016(3)	2.010(3)	2.009(4)
Avg.	2.069	2.051	2.046	2.036	2.031	2.027
PV	11.74(3)	11.41(3)	11.34(3)	11.18(3)	11.10(3)	11.04(3)
QE	1.0046(2)	1.0053(2)	1.0044(2)	1.0043(2)	1.0042(1)	1.0034(1)
AV	13.6(2)	15.9(3)	14.0(2)	13.4(2)	12.9(2)	10.7(2)
M2-O1	2.051(9)	2.043(8)	2.035(7)	2.025(8)	2.024(8)	2.016(8)
M2-O2	2.098(8)	2.089(8)	2.063(7)	2.069(7)	2.045(7)	2.034(7)
M2-O4 ×4	2.089(4)	2.086(4)	2.071(3)	2.068(3)	2.061(3)	2.051(4)
Avg	2.084	2.079	2.064	2.061	2.052	2.042
PV	11.97(4)	11.89(4)	11.63(3)	11.59(3)	11.44(3)	11.27(3)
QE	1.0058(3)	1.0051(2)	1.0050(2)	1.0049(2)	1.0050(2)	1.0052(2)
AV	20.6(5)	18.0(4)	17.7(4)	17.1(4)	17.4(4)	18.2(4)
M3-O1 ×2	2.022(3)	2.008(2)	2.000(2)	1.996(2)	1.989(2)	1.989(2)
M3-O3 ×2	2.122(4)	2.123(4)	2.106(4)	2.097(4)	2.092(4)	2.077(4)
M3-O4 ×2	2.123(3)	2.112(3)	2.102(3)	2.094(3)	2.087(3)	2.075(3)
Avg.	2.089	2.081	2.069	2.062	2.056	2.047
PV	12.04(2)	11.91(2)	11.72(2)	11.60(2)	11.50(2)	11.35(2)
QE	1.0067(2)	1.0067(2)	1.0060(2)	1.0059(2)	1.0059(2)	1.0054(2)
AV	22.0(4)	21.5(4)	19.2(3)	19.2(4)	19.0(4)	17.8(4)
Si-O2	1.701(4)	1.691(4)	1.695(3)	1.685(4)	1.688(3)	1.688(4)
Si-O3	1.637(6)	1.625(6)	1.629(5)	1.630(5)	1.625(5)	1.629(5)
Si-O4 ×2	1.640(3)	1.634(3)	1.625(3)	1.626(3)	1.624(3)	1.624(3)
Avg	1.654	1.646	1.644	1.642	1.640	1.641
PV	2.312(8)	2.279(8)	2.268(7)	2.259(8)	2.254(8)	2.259(8)
QE	1.0038(2)	1.0033(2)	1.0036(2)	1.0035(2)	1.0034(2)	1.0034(2)
AV	15.1(5)	13.0(4)	14.2(3)	14.0(4)	13.3(4)	13.4(5)
			Fe25			
M1-O3 ×2	2.133(6)	2.120(5)	2.100(5)	2.095(6)	2.078(6)	2.074(5)
M1-O4 ×4	2.066(5)	2.061(5)	2.054(4)	2.049(5)	2.051(5)	2.044(4)
Avg	2.088	2.081	2.070	2.065	2.060	2.054
PV	12.04(4)	11.92(4)	11.74(3)	11.65(3)	11.58(3)	11.48(3)
QE	1.0057(2)	1.0055(2)	1.0048(2)	1.0048(2)	1.0044(2)	1.0043(1)
AV	18.0(3)	17.3(3)	15.5(2)	15.5(3)	14.9(3)	14.5(2)
M2-O1	2.049(9)	2.059(6)	2.050(7)	2.054(7)	2.041(8)	2.036(7)
M2-O2	2.111(8)	2.089(6)	2.073(6)	2.062(7)	2.061(7)	2.051(7)
M2-O4 ×4	2.103(5)	2.095(5)	2.078(4)	2.075(5)	2.062(5)	2.053(4)
Avg	2.095	2.088	2.073	2.069	2.058	2.050
PV	12.17(4)	12.05(4)	11.78(3)	11.72(4)	11.54(4)	11.40(3)
QE	1.0054(2)	1.0048(2)	1.0052(2)	1.0053(2)	1.0049(2)	1.0049(2)
AV	18.7(4)	17.1(3)	18.6(3)	19.0(4)	17.6(4)	17.5(3)
M3-O1 ×2	2.043(2)	2.031(2)	2.022(2)	2.019(2)	2.011(2)	2.009(2)
M3-O3 ×2	2.138(5)	2.117(4)	2.111(4)	2.104(5)	2.103(5)	2.097(4)
M3-O4 ×2	2.140(3)	2.132(3)	2.116(3)	2.108(3)	2.103(3)	2.096(2)
Avg	2.107	2.093	2.083	2.077	2.072	2.067
PV	12.35(2)	12.14(2)	11.96(2)	11.86(2)	11.78(2)	11.70(2)
QE	1.0068(2)	1.0056(2)	1.0055(2)	1.0051(2)	1.0050(2)	1.0049(2)
AV	22.3(4)	18.0(3)	17.7(3)	16.7(3)	16.0(3)	16.0(3)
Si-O2	1.701(4)	1.698(4)	1.691(4)	1.690(4)	1.688(4)	1.683(4)
Si-O3	1.634(6)	1.634(5)	1.633(5)	1.625(6)	1.630(6)	1.623(5)
Si-O4 ×2	1.632(5)	1.620(3)	1.621(4)	1.617(4)	1.614(4)	1.616(4)
Avg	1.650	1.643	1.642	1.637	1.636	1.635
PV	2.294(9)	2.266(7)	2.260(8)	2.243(9)	2.237(9)	2.231(8)
QE	1.0032(3)	1.0033(3)	1.0033(2)	1.0034(2)	1.0038(2)	1.0037(2)
AV	12.8(5)	12.4(4)	13.0(4)	13.4(5)	15.0(5)	14.6(5)

Notes: PV = polyhedral volume (A^3); QE = quardratic elongation; AV = angle variance (Robinson et al. 1971).

TABLE 4. Interatomic angles in $(Mg,Fe)_2SiO_4$ wadsleyite at various pressures

P (GPa)	0.00	2.72	5.23	6.80	8.49	10.12
			Fe00			
O3-M1-O4	93.8(1)	94.0(1)	93.8(1)	93.7(1)	93.6(1)	93.3(1)
O3-M1-O4'	86.2(1)	86.0(1)	86.2(1)	86.3(1)	86.4(1)	86.7(1)
O4-M1-O4'	87.0(2)	86.6(2)	87.0(2)	86.9(2)	87.0(2)	87.3(2)
O4-M1-O4'	93.0(2)	93.4(2)	93.0(2)	93.1(2)	93.0(2)	92.7(2)
O1-M2-O4	84.7(1)	85.0(1)	85.1(1)	85.2(1)	85.1(1)	85.0(1)
O2-M2-O4	95.3(1)	95.0(1)	94.9(1)	94.8(1)	94.9(1)	95.0(1)
O4-M2-O4'	90.3(2)	89.9(2)	90.4(2)	90.1(2)	90.0(2)	90.2(2)
O4-M2-O4''	88.7(2)	89.3(2)	88.7(2)	89.1(2)	89.1(2)	88.9(2)
O1-M3-O1	91.5(2)	91.7(1)	91.6(1)	91.6(1)	91.6(1)	91.4(1)
O1-M3-O3	92.7(1)	92.8(1)	92.6(1)	92.5(1)	92.4(1)	92.3(1)
O1-M3-O4'	84.6(2)	85.2(2)	85.2(2)	85.2(2)	85.3(2)	85.1(2)
O1-M3-O4''	97.3(2)	97.3(2)	96.8(2)	97.0(2)	97.0(2)	96.8(2)
O3-M3-O3	84.4(2)	83.9(2)	84.3(2)	84.5(2)	84.5(2)	85.0(2)
O3-M3-O4	91.5(2)	90.9(2)	91.1(2)	90.8(2)	90.8(2)	91.0(2)
O3-M3-O4'	86.5(2)	86.4(2)	86.8(2)	86.8(2)	86.7(2)	87.1(2)
O2-Si-O3	111.4(3)	111.2(3)	110.8(3)	111.3(3)	111.1(3)	111.0(3)
O2-Si-O4	104.4(2)	104.8(2)	104.6(2)	104.7(2)	104.8(2)	104.8(2)
O3-Si-O4	111.6(2)	111.3(2)	111.6(2)	111.4(2)	111.3(2)	111.5(2)
O4-Si-O4'	112.9(2)	113.1(2)	113.1(2)	113.0(2)	113.2(2)	112.9(3)
			Fe25			
O3-M1-O4	94.5(1)	94.3(1)	94.2(1)	94.1(1)	94.2(1)	94.2(1)
O3-M1-O4'	85.5(1)	85.7(1)	85.8(1)	85.9(1)	85.8(1)	85.8(1)
O4-M1-O4	86.8(3)	86.6(3)	87.2(2)	87.1(3)	87.6(3)	87.8(2)
O4-M1-O4'	93.2(3)	93.4(3)	92.8(2)	92.9(3)	92.4(3)	92.2(2)
O1-M2-O4	85.4(1)	85.3(1)	85.1(1)	85.1(1)	85.3(1)	85.3(1)
O2-M2-O4	94.6(1)	94.7(1)	94.9(1)	94.9(1)	94.7(1)	94.7(1)
O4-M2-O4'	91.8(3)	91.4(3)	91.5(2)	91.4(3)	91.8(3)	91.7(2)
O4-M2-O4''	87.4(3)	87.8(3)	87.7(2)	87.7(3)	87.4(3)	87.6(2)
O1-M3-O1	90.8(1)	90.6(1)	90.7(1)	90.5(1)	90.7(1)	90.5(1)
O1-M3-O3	93.2(1)	93.0(1)	92.9(1)	93.0(1)	92.9(1)	92.9(1)
O1-M3-O4	84.2(3)	85.1(2)	84.9(2)	85.1(2)	85.0(2)	84.9(2)
O1-M3-O4'	96.4(3)	95.9(2)	95.9(2)	95.6(2)	95.4(3)	95.4(2)
O3-M3-O3'	84.4(2)	84.6(2)	84.5(2)	84.6(2)	84.4(2)	84.5(2)
O3-M3-O4	92.8(2)	92.3(2)	92.1(2)	92.2(2)	92.0(2)	92.0(2)
O3-M3-O4'	86.6(2)	86.7(2)	87.1(2)	87.1(2)	87.6(2)	87.7(2)
O2-Si-O3	110.9(3)	110.9(3)	110.7(3)	110.7(3)	110.3(3)	110.4(3)
O2-Si-O4	104.7(2)	104.9(3)	104.8(2)	104.7(2)	104.5(2)	104.6(2)
O3-Si-O4	111.7(2)	111.5(2)	111.7(2)	111.8(2)	112.2(2)	112.1(2)
O4-Si-O4'	112.8(3)	112.7(2)	112.6(2)	112.5(3)	112.7(3)	112.7(2)

cation octahedra. This topology provides little opportunity for bending of cation-oxygen-cation angles. Variations of the wadsleyite structure with pressure, therefore, are best analyzed in terms of the sizes and distortion indices of its four symmetrically independent cation-oxygen polyhedra: octahedral M1, M2, and M3, and tetrahedral Si. All Mg-O bonds in all three MgO_6 octahedra display significant compression. Variations of mean Mg-O distances for the three octahedra (Fig. 1) are the same within experimental error, yielding average linear compressibilities of 0.0023(1), 0.0024(2), and 0.0022(1)/GPa for Mg-O bonds in M1, M2, and M3, respectively. The tetrahedron is significantly more rigid, with mean Si-O compressibility of 0.00095/GPa. Corresponding polyhedral bulk moduli are 146(8), 137(13), 149(7), and 350(60) GPa for M1, M2, M3, and Si, respectively. These values are similar to the average polyhedral bulk moduli of Mg_2SiO_4 forsterite: ≈130 GPa for Mg octahedra and >300 GPa for Si tetrahedra, as reported by Hazen and Finger (1980).

Individual Mg-O bonds display significant differences in their compressibilities. In the M1 octahedron, for example, the compressibilities of two longer M1-O3 bonds, which are roughly parallel to the *c* axis, are 0.0028(2)/GPa. Note that O3 is significantly overbonded, to two Si and one M1—a situation that often results in relatively long, weak, and compressible bonds. By contrast, the compressibilities of four shorter M1-O4 bonds, roughly perpendicular to the *c* axis, are 0.0016(2)/GPa. The polyhedral distortion indices of the M1 octahedron decrease slightly as a consequence of this differential compression.

A similar situation obtains for the M2 octahedron. The compressibility of the longest Mg-O bond, M2-O2, which is strictly parallel to the *c* axis, is 0.0030(2)/GPa, compared to the 0.0018/GPa value for four M2-O4 bonds and 0.0017/GPa for one M2-O1 bond. As in the M1 octahedron, the polyhedral distortion indices decrease slightly, reflecting the increased regularity of the bond distances.

Likewise for M3, two M3-O4 bonds which are approximately parallel to the *c* axis are also the longest and most compressible Mg-O bonds [0.0022(2)/GPa], compared to 0.0016 and 0.0021 for two M3-O1 and two M3-O3 bonds, respectively. Once again, polyhedral distortion indices decrease slightly with pressure.

These differences in individual octahedral bond compressibilities contribute significantly to the anisotropic compression of the wadsleyite unit cell. In all three octahedra, bonds approximately parallel to the *c* axis are most compressible. In contrast to bond distances, all of which display significant compression, no significant changes (i.e., variations > ±0.5°) are observed for any of the internal O-Mg-O octahedral angles.

Individual silicate tetrahedra are relatively incompressible compared to octahedra, and they behave as rigid structural units. The Si_2O_7 dimer, however, is somewhat flexible at the O2 bridging atom, as measured by the Si-O2-Si angle. This angle decreases by 1.4°, from 122.4(4)° to 121.0(4)°, between 0 and 10.12 GPa. This decrease in Si-O-Si angle with pressure is analogous to the angle bending that occurs in many framework silicates with increasing pressure (e.g., Hazen and Finger 1985).

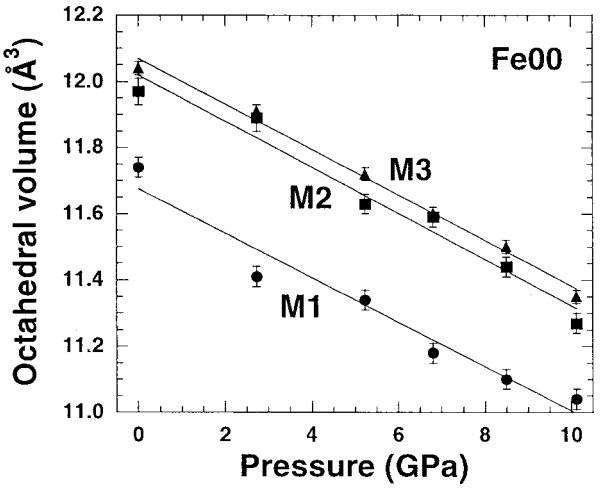

FIGURE 1. Octahedral volumes versus pressure for the M1, M2, and M3 sites of β-Mg_2SiO_4.

Structural variations of Fe25 wadsleyite

Structural variations of Fe25 wadsleyite with pressure are, in most respects, qualitatively similar to those of Fe00. As in Fe00, the octahedral (Mg,Fe)-O bonds that are roughly parallel to the *c* axis are, in all cases, both the longest and the most compressible. Furthermore, distortion indices in all three octahedra decrease with increasing pressure. As in Fe00, the silicate tetrahedron of Fe25 acts as a rigid unit, while the Si-O2-Si angle of the silicate dimer decreases from 121.4(5)° to 120.7(4)°.

The high-pressure behaviors of Fe00 and Fe25 wadsleyites differ in at least one important respect, however. In the Mg end member, the three octahedra display the same bulk moduli within experimental error:146(8), 137(13), and 149(7) GPa for M1, M2, and M3, respectively. In Fe25, by contrast, octahedral bulk moduli differ significantly (Fig. 2): values are 188(15), 126(10), and 166(6) GPa for these three octahedra, respectively. These differences correlate with Mg-Fe ordering in a curious way. In most instances of Mg-Fe solid solution, end members with longer Fe^{2+}-O distances tend to be more compressible than those with shorter Mg-O bonds (Hazen 1993), in accord with bulk modulus-volume systematics for cation-anion polyhedra (e.g., Hazen and Finger 1982). By contrast, in wadsleyite the relatively Mg-rich M2 octahedron, with a refined composition of $(Mg_{0.87}Fe_{0.13})$, is significantly more compressible than octahedra of end-member β-Mg_2SiO_4. M2 is also significantly more compressible than the relatively Fe-enriched M1 and M3 octahedra, which both have compositions of ~$(Mg_{0.71}Fe_{0.29})$. Possible reasons for this anomaly are considered in the following section.

Fe-Mg ordering in wadsleyite

The tendency for Fe to occupy M1 and M3 preferentially over M2 has been well documented, but poorly understood. In Fe-Mg silicates iron typically prefers larger octahedral sites, with a secondary tendency to partition into more distorted octahedra as a result of crystal field splitting energy. However, Finger et al. (1993) noted that the observed ordering sequence for Fe: M3 ≥ M1 >> M2 correlates with neither the room-pressure polyhedral volumes, nor with the octahedral distortion parameters. In both Fe00 and Fe25, M3 is the largest and most distorted site, and so one can rationalize its Fe enrichment. But at room pressure M1 in both Fe00 and Fe25 is smaller than M2, while octahedral distortions are greater or equal in M2, depending on composition. Thus, based on room-pressure data alone, there is no obvious reason why Fe should prefer M1 over M2.

A possible explanation for concentration of Fe in M1 relative to M2 is revealed by the fact that M2 is significantly more compressible than M1. At room pressure the M1 octahedron of Fe25 is smaller than M2, but their volumes cross over at about 8 GPa and above that pressure M2 is the smallest octahedron (Fig. 2). Temperature variations of the structure of an Fe-bearing wadsleyite have yet to be determined, but it seems likely that at the conditions of Fe25 synthesis (15.5 GPa and 1800 °C) M1 is significantly larger than M2, and thus the more likely repository for iron. Fe-Mg distribution in wadsleyite, therefore, may represent an example of pressure-induced ordering (Hazen and Navrotsky 1996), and site occupancies may be a function of synthesis conditions. Investigation of the structure of Fe-bearing wadsleyite in situ at high pressure and temperature would be especially useful in this regard.

In spite of this plausible explanation for the observed Mg-Fe ordering, the question remains why the presence of 25% Fe in octahedral sites should so dramatically alter the details of polyhedral compression. In Fe00, all three octahedra have bulk moduli consistent with 144 ± 6 GPa. The Fe-enriched M1 and M3 octahedra of Fe25, however, are much stiffer, with average bulk moduli more than 20% greater. These anomalous values are inconsistent with polyhedral bulk modulus-volume systematics. [Significant Fe^{3+} could increase the octahedral bulk moduli of wadsleyite, but Mössbauer spectroscopic analysis (Finger et al. 1993) indicates the presence of only minor ferric iron in this sample.]

One possible explanation for the relative incompressibility of Fe-enriched M1 and M3 in Fe25 wadsleyite is related to the observation that 25% Fe is close to the maximum Fe content stable in β-$(Mg,Fe)_2SiO_4$ at the high pressure of synthesis. The relatively rigid Si_2O_7 dimer constrains the size of adjacent edge-sharing octahedra. Consequently, the average room-pressure octahedral M-O distance in Fe25 wadsleyite (correcting for bond and site multiplicities) is 2.100 Å, which is unusually short for an average composition of $(Mg_{0.75}Fe_{0.25})$. By contrast, the average M-O octahedral distance in an olivine of the same composition is 2.126 Å. Perhaps under decompression, as Mg-Fe octahedra attempt to expand significantly more than silicate tetrahedra, the structure becomes internally strained owing to polyhedral misfit. Fe-enriched sites become, in effect, "overstuffed" under decompression, and thus are anomalously stiff compared to Fe sites in lower-pressure phases like olivine. This anomalous stiffening of polyhedra with the largest (and intrinsically most compressible) cations, may represent an intermediate decompression behavior. At the extreme, such differential polyhedral expansion on decompression can lead to internal

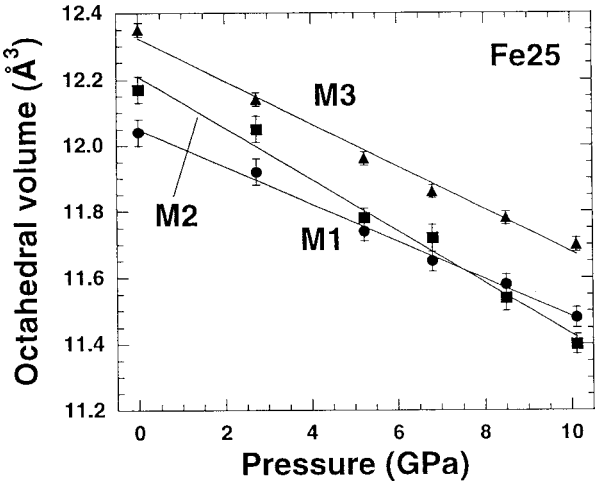

FIGURE 2. Octahedral volumes versus pressure for the M1, M2, and M3 sites of β-$(Mg_{0.75}Fe_{0.25})_2SiO_4$. Note the volume cross-over of M1 and M2 at ~8 GPa.

strains sufficient to disrupt the crystalline structure, as in the case of decompression amorphization of $CaSiO_3$ perovskite (Liu and Ringwood 1975).

CONCLUSIONS

This investigation of the wadsleyite structure at high pressure reinforces some of the most general trends observed in other orthosilicate studies. As in other high-pressure structural investigations of orthosilicates, including olivines, silicate spinels, zircon, garnets, and aluminosilicates, silicate tetrahedra behave as relatively rigid structural units with polyhedral bulk moduli >300 GPa, while larger cation polyhedra are more compressible and dictate the bulk modulus of the crystal. As in other studies, changes in octahedral and tetrahedral distortion indices are relatively small in the room pressure to 10 GPa range. And, as has been often documented in other structures, angles between corner-linked polyhedra, such as the Si-O2-Si angle in wadsleyite, decrease significantly more with pressure than other M-O-M angles.

But this work also reveals complexities not easily explained by prevailing high-pressure crystal-chemical systematics, which have been formulated primarily from data on crystals stable at crustal pressures. The seemingly anomalous compressibilities of the Fe-enriched M1 and M3 sites of Fe25 wadsleyite, along with similar anomalies in Mg-Fe silicate spinels (Hazen 1993), point to the need for additional studies. High-pressure structure investigations should be conducted on other crystals quenched metastably from high pressure. Such quenched phases might also display anomalously incompressible "over-stuffed" polyhedra. By the same token, the structures and elastic properties of wadsleyite and other high-pressure phases need to be examined in situ, in their high-pressure and high-temperature regions of stability. At such conditions, differential thermal expansion and compression of constituent polyhedra may lead to reduced internal strain, which, in turn, might result in modified elastic moduli that are more appropriate to evaluating models of Earth's deep interior.

ACKNOWLEDGMENTS

We gratefully acknowledge the synthesis of wadsleyite single crystals at the Stony Brook High-Pressure Laboratory, which is jointly sponsored by the NSF Center for High Pressure Research and the State University of New York. Two anonymous reviewers provided valuable suggestions and corrections. X-ray diffraction studies at the Geophysical Laboratory are supported by NSF grant EAR-9805282, the Center for High Pressure Research, and by the Carnegie Institution of Washington. M.B.W. is grateful for the Geophysical Laboratory's Summer Internship Program, which is sponsored by the Carnegie Institution and NSF.

REFERENCES CITED

Anderson, D.L. (1970) Petrology of the mantle. Mineralogical Society of America Special paper, 3, 85–93.

Becker, P.J. and Coppens, P. (1975) Extinction within the limit of validity of the Darwin transfer equations: III. Non-spherical crystals and anisotropy of extinction. Acta Crystallographica, A31, 417–425.

Bell, D.R. and Rossman, G.R. (1992) Water in Earth's mantle: The role of nominally anhydrous minerals. Science, 255, 1391–1396.

Bina, C.R. and Wood, B.J. (1987) Olivine-spinel transitions: experimental and thermodynamic constraints and implications for the nature of the 400-km seismic discontinuity. Journal of Geophysical Research, 92, 4853–4866.

Chopelas, A. (1991) Thermal properties of β-Mg_2SiO_4 (modified spinel at mantle pressures derived from vibrational spectroscopy: Implications for the mantle at 400 km. Journal of Geophysical Research, 96, 11817–11830.

Cynn, H. and Hofmeister, A.M. (1994) High-pressure IR spectra of lattice modes and OH vibrations in Fe-bearing wadsleyite. Journal of Geophysical Research, 99, 17717–17727.

Downs, J.W. (1989) Possible sites for protonation in β-Mg_2SiO_4 from an experimentally derived electrostatic potential. American Mineralogist, 74, 1124–1129.

Fei, Y., Mao, H-K., Shu, J., Parthasarathy, G., Bassett, W.A., and Ko, J. (1992) Simultaneous high-P and high-T X-ray diffraction study of β-$(Mg,Fe)_2SiO_4$ to 26 GPa and 900 K. Journal of Geophysical Research, 97, 4489–4495.

Finger, L.W. and King, H. (1978) A revised method of operation of the single-crystal diamond cell and refinement of the structure of NaCl at 32 kbar. American Mineralogist, 63, 337–342.

Finger, L.W. and Prince, E. (1975) A system of FORTRAN IV computer programs for crystal structure computations. National Bureau of Standards Technology Note 854.

Finger, L.W., Hazen, R.M., Zhang, J., Ko, J., and Navrotsky, A. (1993) The effect of Fe on the crystal structure of wadsleyite, β-$(Mg_{1-x}Fe_x)_2SiO_4$, $0.00 < x < 0.40$. Physics and Chemistry of Minerals, 19, 361–368.

Gasparik, T. (1993) The role of volatiles in the transition zone. Journal of Geophysical Research, 98, 4287–4299.

Gwanmesia, G.D., Rigden, S., Jackson, I., and Liebermann, R.C. (1990) Pressure dependence of elastic wave velocity for β-Mg_2SiO_4, and the composition of the Earth's mantle. Science, 250, 794–797.

Haiber, M., Ballone, P., and Parrinello, M. (1997) Structure and dynamics of protonated Mg_2SiO_4: An ab-initio molecular dynamics study. American Mineralogist, 82, 913–922.

Hazen, R.M. (1993) Comparative compressibilities of silicate spinels: Anomalous behavior of $(Mg,Fe)_2SiO_4$. Science, 259, 206–209.

Hazen, R.M. and Finger, L.W. (1980) Crystal structure of forsterite at 40 kbar. Carnegie Institution of Washington Year Book 79, 346–367.

———(1982) Comparative Crystal Chemistry. Wiley, New York.

———(1985) Crystals at high pressure. Scientific American, 252, 110–117.

Hazen, R.M. and Navrotsky, A. (1996) Effects of pressure on order-disorder reactions. American Mineralogist, 81, 1021–1035.

Hazen, R.M., Zhang, J., and Ko, J. (1990) Effects of Fe/Mg on the compressibility of synthetic wadsleyite: β-$(Mg_{1-x}Fe_x)_2SiO_4$, $0.00\ (x < 0.25)$. Physics and Chemistry of Minerals, 17, 416–419.

Horiuchi, H. and Sawamoto, H. (1981) β-Mg_2SiO_4: single-crystal X-ray diffraction study. American Mineralogist, 66, 568–575.

Ibers, J.A. and Hamilton, W.C. (1974) International tables for X-ray crystallography. Vol. IV, 366 p. Kynoch, Birmingham, U.K.

Inoue, T. (1994) Effect of water on melting phase-relations and melt composition in the system Mg_2SiO_4-$MgSiO_3$-H_2O up to 15 GPa. Physics of the Earth and Planetary Interiors, 85, 237–245.

Jeanloz, R. and Hazen, R.M. (1991) Finite-strain analysis of relative compressibilities: Applications to the high-pressure wadsleyite phase as an illustration. American Mineralogist, 76, 1765–1768.

Jeanloz, R. and Thompson, A.B. (1983) Phase transition and mantle discontinuities. Reviews in Geophysics and Space Physics, 21, 51–74.

King, H.E. and Finger, L.W. (1979) Diffracted beam crystal centering and its application to high pressure crystallography. Journal of Applied Crystallography, 12, 374–378.

Kudoh, Y. and Inoue, T. (1999) Mg-vacant structural modules and dilution of the symmetry of hydrous wadsleyite, β-$Mg_{2-x}SiH_{2x}O_4$ with $0.00 \le x \le 0.25$. Physics and Chemistry of Minerals, 26, 382–388.

Kudoh, Y., Inoue, T., and Arashi, H. (1996) Structure and crystal chemistry of hydrous wadsleyite $Mg_{1.75}SiH_{0.5}O_4$: Possible hydrous magnesium silicate in the mantle transition zone. Physics and Chemistry of Minerals, 23, 461–469.

Lehmann, M.S. and Larsen, F.K. (1974) A method for location of the peaks in step-scan-measured Bragg reflexions. Acta Crystallographica, A30, 580–584.

Li, B., Gwanmesia, G.D., and Liebermann, R.C. (1996) Sound velocity of olivine and beta polymorphs of Mg_2SiO_4 at Earth's transition zone pressures. Geophysical Research Letters, 23, 2259–2262.

Li, B., Liebermann, R.C., and Weidner, D.J. (1998) Elastic moduli of wadsleyite (β-Mg_2SiO_4) to 7 gigapascals and 873 Kelvin. Science, 281, 675–677.

Liu, L.G. and Ringwood, A.E. (1975) Synthesis of a perovskite-type polymorph of $CaSiO_3$. Earth and Planetary Science Letters, 28, 209–211.

Mao, H.K., Xu, J., and Bell, P.M. (1986) Calibration of the ruby pressure gauge to 800 kbar under quasi-hydrostatic conditions. Journal of Geophysical Research, 91, 4673–4676.

McMillan, P.F., Akaogi, M., Sato, R.K., Poe, B., and Foley, J. (1991) Hydroxyl groups in β-Mg_2SiO_4. American Mineralogist, 76, 354–360.

Mizukami, S., Ohtani, A., and Kawai, N. (1975) High-pressure X-ray diffraction studies on β- and g-Mg_2SiO_4. Physics of the Earth and Planetary Interiors, 10, 177–182.

Moore, P.B. and Smith, J.V. (1970) Crystal structure of β-Mg_2SiO_4: Crystal-chemical and geophysical implications. Physics of the Earth and Planetary Interiors, 3, 166–177.

Morimoto, N., Akimoto, S., Koto, K., and Tokonami, M. (1969) Modified spinel, beta-manganous orthogermanate: stability and crystal structure. Science, 165, 586–588.

Morimoto, N., Akimoto, S., Koto, K., and Tokonami, M. (1970) Crystal structures of high pressure modifications of Mn_2GeO_4 and Co_2GeO_4. Physics of Earth and Planetary Interiors, 3, 161–165.

Morimoto, N., Tokonami, M., Watanabe, M., and Koto, K. (1974) Crystal structures of three polymorphs of Co_2SiO_4. American Mineralogist, 59, 475–485.

Reynard, B., Takir, F., Guyot, F., Gwanmesia, G.D., Liebermann, R.C., and Gillet, P. (1996) High-temperature Raman spectroscopic and X-ray diffraction study of β-Mg_2SiO_4: Insights into its high-temperature thermodynamic properties and the β- to α-phase-transition mechanism and kinetics. American Mineralogist, 81, 585–594.

Robinson, K., Gibbs, G.V., and Ribbe, P.H. (1971) Quadratic elongation: A quantitative measure of distortion in coordination polyhedra. Science, 172, 567–570.

Sawamoto, H. and Horiuchi, H. (1990) β-$(Mg_{0.9}Fe_{0.1})_2SiO_4$: Single crystal structure, cation distribution, and properties of coordination polyhedra. Physics and Chemistry of Minerals, 17, 293–300.

Sawamoto, H., Weidner, D.J., Sasaki, S., and Kumazawa, M. (1984) Single-crystal elastic properties of modified spinel (beta) phase of magnesium orthosilicate. Science, 224, 749–751.

Smyth, J.R. (1987) β-Mg_2SiO_4: a potential host for water in the mantle? American Mineralogist, 72, 1051–1055.

Smyth, J.R. (1994) A crystallographic model for hydrous wadsleyite (β-Mg_2SiO_4): an ocean in the Earth's interior? American Mineralogist, 79, 1021–1024.

Smyth, J.R., Kawamoto, T., Jacobsen, S.D., Swope, R.J., Hervig, R.L., and Holloway, J.R. (1997) Crystal Structure of monoclinic hydrous wadsleyite [β-$(Mg,Fe)_2SiO_4$]. American Mineralogist, 82, 270–275.

Tsukimura, K., Sato-Sorenson, Y., Ghose, S., and Sawamoto, H. (1988) High-temperature single-crystal study of β-Mg_2SiO_4. Eos, 69, 498.

Willians, Q., Jeanloz, R., and Akaogi, M. (1986) Infrared vibrational spectra of beta-phase Mg_2SiO_4 and Co_2SiO_4 to pressures of 27 GPa. Physics and Chemistry of Minerals, 13, 141–145.

Woodland, A.B. and Angel, R.J. (1998) Crystal structure of a new spinelloid with the wadsleyite structure in the system Fe_2SiO_4-Fe_3O_4 and implications for the Earth's mantle. American Mineralogist, 83, 404–408.

Young, T.E., Green, H.W., Hofmeister, A.M., and Walker, D. (1993) Infrared spectroscopic investigation of hydroxyl in β-$(Mg,Fe)_2SiO_4$ and coexisting olivine: implications for mantle evolution and dynamics. Physics and Chemistry of Minerals, 19, 409–422.

Zha, C-S., Duffy, T.S., Mao, H-K, Downs, R.T., Hemley, R.J., and Weidner, D.J. (1997) Single-crystal elasticity of β-Mg_2SiO_4 to the pressure of the 410 km seismic discontinuity in the Earth's mantle. Earth and Planetary Science Letters, 147, 9–15.

MANUSCRIPT RECEIVED JUNE 21, 1999
MANUSCRIPT ACCEPTED DECEMBER 17, 1999
PAPER HANDLED BY JAMES W. DOWNS